Tunneling spectroscopy of the superconducting gap in MgB_2

Toshikazu Ekino,[1,2,*] Tomoaki Takasaki,[2] Takahiro Muranaka,[3] Jun Akimitsu,[3] and Hironobu Fujii[1,2]
[1]*Faculty of Integrated Arts and Sciences, Hiroshima University, Higashi-Hiroshima 739-8521, Japan*
[2]*Graduate School of Advanced Sciences of Matter, Hiroshima University, Higashi-Hiroshima 739-8526, Japan*
[3]*Department of Physics, Aoyama-Gakuin University, 6-16-1, Chitosedai, Setagaya, Tokyo 157-8572, Japan*
(Received 30 December 2002; published 14 March 2003)

The tunneling technique with a break junction has been applied to investigate the multiple superconducting gaps in MgB_2. The observed gap features can be explained by combining inherent and induced order parameters. The largest gap of $\Delta=9-10$ meV corresponds to a very strong-coupling ratio $2\Delta/k_BT_c=5-6$. Upon warming, this gap decreases in accordance with the BCS dependence, while the smaller gaps reduce faster than that but persist up to T_c. Therefore, the smallest gap of $\Delta=2-2.5$ meV gives $2\Delta/k_BT_c=1.2-1.5$. The magnetic field can distinguish the behavior of the gap. The extrapolated highest gap-closing field for the largest gap agrees with the upper-critical field, thereby indicating that this gap is predominant to MgB_2.

DOI: 10.1103/PhysRevB.67.094504 PACS number(s): 74.50.+r, 74.25.Jb, 74.70.Ad

Among numbers of experiments on the simple binary superconductor MgB_2 with $T_c=39$ K,[1] there have been emerging serious discrepancies, namely, the observations of either single-gap or two-gap features in the spectral response.[2–8] For example, high-resolution photoemission spectroscopy (PES) on the burnished surface showed a single gap, whereas that on cleaved surface showed the two-gap feature.[3,4] Raman-scattering measurements also indicated either the two-gap state,[9] or the slightly anisotropic single gap.[10] The origin of the two-gap feature on the one hand, is attributed to the multiband superconductivity consisting of boron two-dimensional (2D) p_{xy} and 3D p_z bands.[11] Such a multigap feature, though the situation is different, was previously introduced theoretically.[12] On the other hands, alternative explanations can also be given on the basis of the proximity effect or the gap anisotropy.[13,14]

In this paper, we report electron-tunneling measurements on a MgB_2 polycrystal using a superconductor-insulator-superconductor (SIS) break junction to investigate the multigap features. Electron-tunneling spectroscopy provides the most direct probe to measure the energy gap 2Δ through the measurements of current (I)–voltage (V) characteristics of the junction. The key observations are the strong-coupling gap of $\Delta\sim10$ meV and the non-BCS T dependence of the smaller gaps having 2–6 meV with single T_c, which can arise from the induced superconductivity owing to the band multiplicity or the proximity effect. The extrapolated gap-closing field for the largest gap is consistent with the upper critical field of MgB_2.[15]

The polycrystalline samples were synthesized from a mixture of $3N$ Mg powder and $2N$ amorphous B at 973 K in 200-atm Ar gas for 10 h, followed by annealing at 1623 K under 5.5-G Pa.[1] It shows a resistive transition at $T_c=39.2$ K with a width 0.5 K and a sharp onset in the susceptibility with a perfect flux exclusion at 4.2 K. The residual resistance ratio between 300 and 40 K reaches $\approx3.6-4.1$ for the most sample batches. Tunneling measurements were done with a four-probe, *in situ* SIS break junction. The cracked junction interface monitored by scanning electron microscopy revealed a grain size of $\sim1-3\mu$m showing thin platelets, which reflects the formation of microcrystals. The existence of oxygen was confirmed by the energy-dispersion X-ray analysis of the cleaved fresh surface.[16]

Figure 1 shows a series of the representative tunneling conductance curves at 4.2 K. The data were taken from different junctions. The intensive gap peaks and nearly bias-independent background conductance indicate high barrier height and transparency. In Figs. 1(a) and 1(b), the intensities of the outer-bias structures are largely different from each other, but they exhibit predominant peaks at $\approx\pm4-5$ mV. A relatively low junction resistance and a weak Josephson peak with well-pronounced outer humps suggest a narrower tunneling barrier. The *peak-to-peak* separations of the apparent gap edge are $V_{p\text{-}p}\approx8$ mV [(a) and (b)], ≈20 mV [(b) and (d)], and ≈40 mV (c). Note that these gaps exhibit *the same* T_c. These multigap features can be explained in terms of the proximity effect[13] or the multiband superconductivity[11] with the anisotropic gap.[14] Assuming the anisotropic gap, the broadened conductance feature should be observed as a result of averaging out of the momentum ($\mathbf{k}$) distribution of the gap. In this case, the multigap feature with no-leakage conductance around zero bias as in (a) could be hardly observed. To fit the experimental conductance to the calculated one, we assumed a superconducting-normal bilayer tunneling model of the proximity effect.[13] This is a similar expression to the two-band model.[12] The physical difference between them is that the former involves a spatially separated region, while for the latter the separation of the charge transfer in the $\mathbf{k}$ space is essential. In both cases, there exist gap parameters Δ_1 and Δ_2 ($\Delta_1>\Delta_2$), which are correlated to each other. The expression involving these correlated gaps is

$$\Delta_i=(\Delta_i^0+\Gamma_i\Delta_j/[\Delta_j^2-E^2]^{1/2})(1+\Gamma_j/[\Delta_j^2-E^2]^{1/2})^{-1/2},\quad [i,j(\neq i)]=1,2,$$

with a small broadening parameter in E, where Δ_i^0 is a BCS potential for the inherent pairing interaction, and Γ_i is the penetrating rate or the interband scattering rate for the proximity effect or the two-band model, respectively. The calculation is done by iteration until Δ_1 and Δ_2 in the two equations become consistent with each other. In Figs. 1(a), 1(b), and 1(d), the broken curves represent the calculated SIS tun-

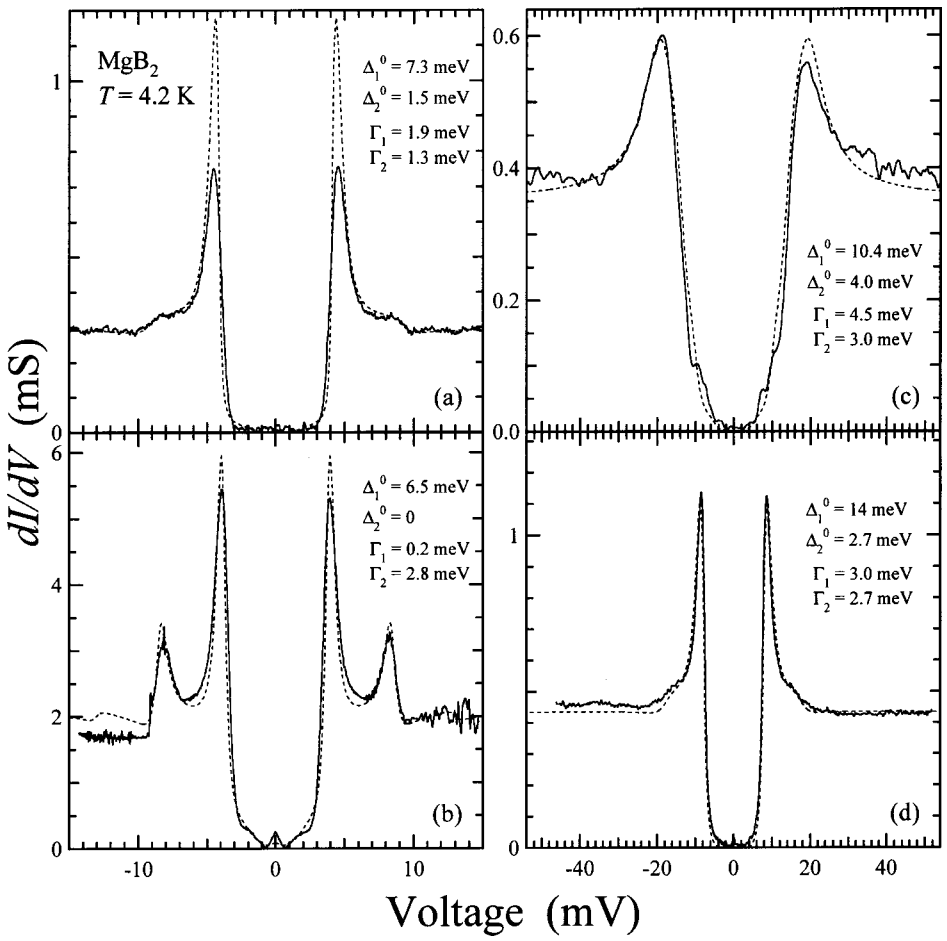

FIG. 1. Tunneling conductance for MgB_2 break junctions at 4.2 K. The broken curves represent the calculated density of states with Δ_2 [(a), (b), and (d)] and with Δ_1 (c) using the correlated two-gap (proximity effect) model (see the text).

neling conductance with the predominant smaller gap Δ_2. The calculated curves almost agree with the experimental data. This indicates that the outer humps and peaks are due to the gap-edge crossing consisting of Δ_1 and Δ_2 in the SIS junction. For (a) and (b), almost common values of $\Delta_1^0 = 6.9 \pm 0.4$ meV are obtained. The no leakage conductance bottom of (a) reflects a nonzero value of Δ_2^0. On the other hand, no inherent pairing potential in the induced part is suggested in (b) by $\Delta_2^0 = 0$. In spite of this difference, the values of $\Delta_2^0 + \Gamma_2 = 2.8$ meV in both (a) and (b) are consistent with each other, which yields the similar inner gap-peak positions.[13] Figure 1(c) shows a broadened large-gap structure, which can be fitted by the density of states for the larger gap (Δ_1). The existence of Δ_2 nested in Δ_1 inevitably fits the data better, thereby indicating that the correlated two-gap (proximity tunneling) model is suitable even for this large gap. Significantly, the $\Delta_1^0 \sim 10$ meV in (c) is much larger than that of (a) and (b). We have also observed a signature of the large gap in the predominant small gap (Δ_2) spectrum, as shown in (d). In (c) and (d), the values $\Delta_2^0 + \Gamma_2 = 6.3 \pm 0.7$ meV are close to Δ_1^0 of (a) and (b), thereby demonstrating an inherent systematic feature of the induced order parameter.

The T evolution of the tunneling conductance for the largest gap like in Fig. 1(c) is shown in Fig. 2. $T_c \approx 39$ K can be determined by the T dependence of the zero-bias conductance (ZBC) (except for the ZB peak) (the right inset). The

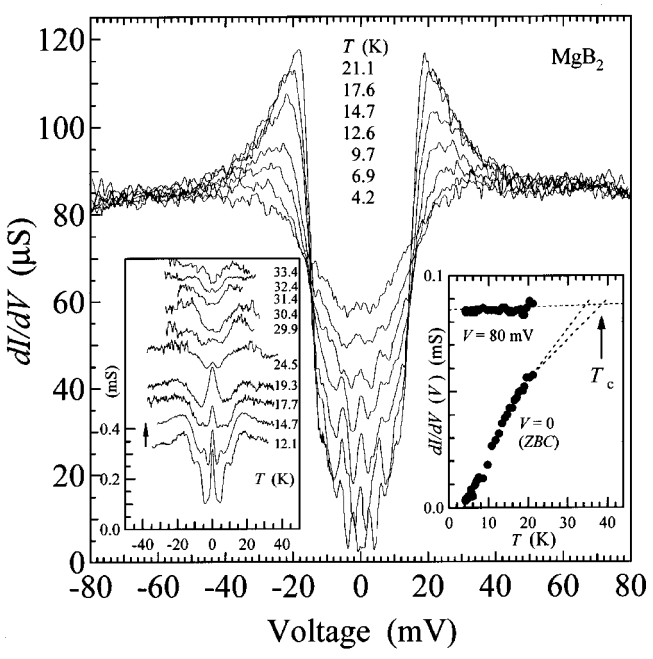

FIG. 2. T variations of the tunneling conductance with the largest gap $\Delta = 9-10$ meV. Right inset: the T dependence of the conductance at $V = 0$ (ZBC) and 80 meV. Left inset: T variations of another SIS tunneling conductance.

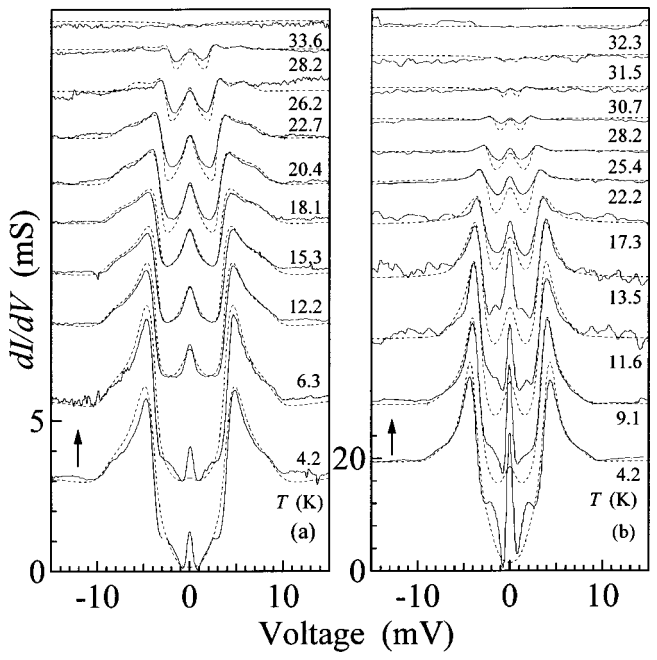

FIG. 3. T variations of the tunneling conductance with the smallest gap. The data of (a) and (b) are taken from the different junctions. The dotted curves represent the calculations by the correlated two-gap model (see the text).

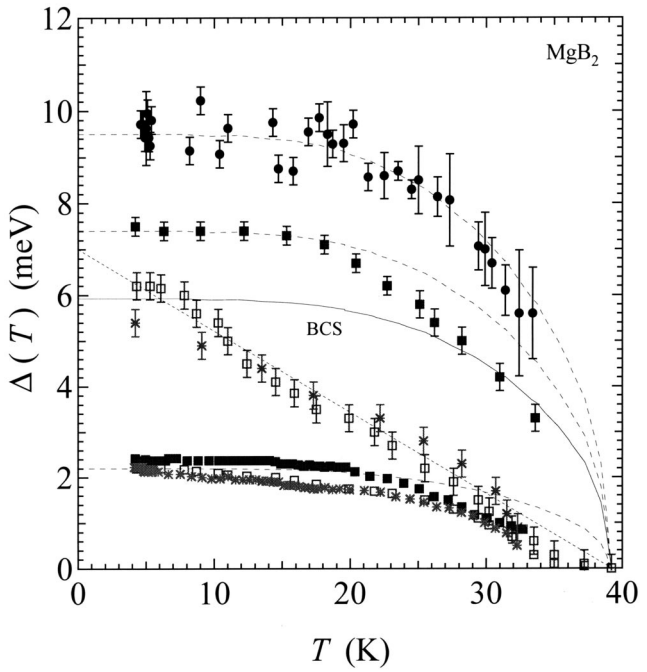

FIG. 4. T dependence of the energy gap Δ (T). For the Δ (4 K)$\approx$6–7.5 and 2–2.5 meV gaps; closed and open squares correspond to the data of Figs. 3(a) and 3(b), respectively. The asterisks are taken from the other junction to demonstrate the reproducibility. The thin solid curve represents a normal BCS prediction with $T_c = 39$ K, while the broken curves are the scaled ones. The broken straight line gives a simple linear extrapolation.

low-bias fine structures probably reflect the smaller gaps shown in Fig. 1. The increased broadening upon warming is due to the thermal transfer of the spectral weight accompanying the increasing quasiparticle scattering. The left inset shows the T evolution of a similar gap size from another junction with distinct gap features at higher T, which indicates the bulk nature of the largest gap. The T variations of the smaller gap are shown in Fig. 3 from two different break junctions, where outer humps are commonly observed at low T. The distinct gap feature exists up to near T_c for both (a) and (b). The humps are visible up to high T for (a), while those for (b) are rapidly obscured upon warming. The broken curves in Fig. 3 represent the fitting results using the above correlated two-gap model.[13] In particular, the calculated curves for (a) explain the observed spectral shapes almost perfectly at any temperatures up to T_c. The substantial deviation at low biases is seen in (b) [and (a) at low T]. The small deviations are also seen for the outer humps. These disagreements may be related to the complex tunneling process such as two-particle tunneling, because the biases of the subgap peaks or shoulders at low T are exactly half the value of biases of the main-gap peaks. It should be possible to reduce these disagreements by introducing additional intergap coupling parameters. Figure 3 demonstrates the reproducible outer humps and/or shoulders by calculations using the known correlated two-gap model even at high temperatures near T_c.[13] The fitted parameters at 4.2 K are $\Delta_1^0 = 7.5(6.4)$ meV, $\Gamma_1 = 3(1.2)$ meV, $\Delta_2^0 = 0.5(1.6)$ meV, and $\Gamma_2 = 3.2(0.9)$ meV for (a) [(b)]. $\Delta_1^0 \approx 6.4$–7.5 meV is noted to be consistent with that of Figs. 1(a) and (b).

Figure 4 shows the T dependence of the gap parameter $\Delta(T)$. For the middle [$\approx$6–7.5 meV (at 4 K)] gaps, $\Delta(T)$ is obtained from the conductance fitting, while that of the largest ($\approx$9–10 meV) and smallest (2–2.5 meV) gaps is obtained by either the peak positions or the fittings. All the data converge at single $T_c \approx 39$ K, regardless of the gap size and its low-T behavior. For the largest gap, it almost agrees with the BCS Δ (T). It is remarkable that the middle size (7.5 meV) gap starts to deviate form the BCS Δ (T) at $\approx$20 K, while another middle gap ($\approx$6 meV) undergoes an almost linear T dependence that is extrapolated to the value close to 7.5 meV at 0 K. The latter feature, which is similar to the PES results,[4] resembles the proximity-induced gap found in the conventional superconductor.[17] The deviation from the BCS curve at high T can also be seen in the smallest 2–2.5 meV gap, but it never exhibits a linear decrease unlike the 6-meV gap. From these facts, at least the middle gap is suggested to arise from a proximity-induced origin.[17]

The largest gap ratio $2\Delta/k_B T_c = 5$–6 for the $\Delta \approx 9-10$ meV gap is consistent with the tunneling data by Bugoslavsky *et al.*[8] and the NMR data,[2] but inconsistent with the other tunneling and PES measurements having a BCS size or less.[3–7] By adopting the relationship $2\Delta/k_B T_c = 3.5\ \{1 + 12.5(k_B T_c / E_{\ln})^2 \ln(E_{\ln}/2\, k_B T_c)\}$ for the isotropic, single-band strong-coupling superconductor,[18] the ratio >5 implies the logarithmic average energy of $E_{\ln} < 10$–15 meV. This is much lower than $E_{\ln} \approx 58$ meV of the inelastic neutron experiment.[19] This discrepancy indicates the difference between the bare phonon density of states and electron-coupled phonon spectrum, which can be related to

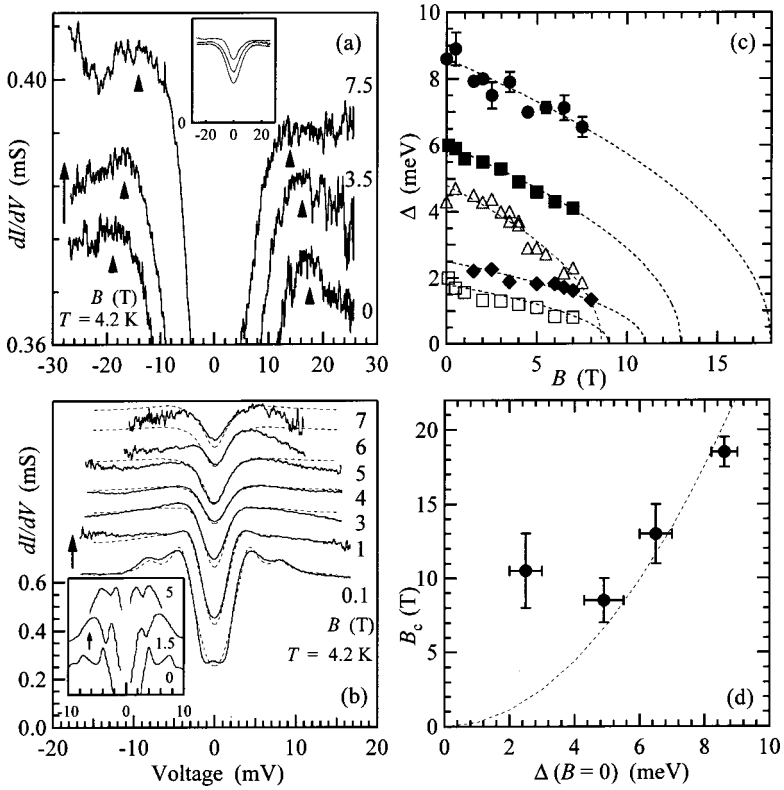

FIG. 5. (a) Magnetic-field evolution of the largest single gap. Inset: the overall conductance features. (b) Magnetic-field evolution of the two-gap feature. The broken curves represent the fitting results (see the text). Inset: apparent multigap feature under the field. (c) Magnetic-field dependence of the gap value. The broken curves represent $\Delta(B)=\Delta(B=0)\,[1-B/B_c]^{1/2}$, (d) The gap-closing field B_c vs the zero-field gap value $\Delta(B=0)$. The broken curve represents $B_c \propto \Delta^2$.

the anisotropic nature of the electron-phonon interaction.[11,20] Since MgB_2 possesses multiple Fermi surfaces consisting of boron $p_{x,y}$ and p_z bands, different gaps could coexist in the clean limit.[11] Since the $p_{x,y}$ band more strongly contributes to the Fermi-surface state density, a strong electron-phonon interaction and a large energy gap can be in fact realized. It should be noted that the gap ratio 5–6 obtained here coincides well with that of the layered nitride superconductor with $T_c=26$ K.[21] The above gap ratio does not seems to be a marginal extension of the conventional strong-coupling feature because of no such a large ratio in the superconductors except for copper-oxides.[22]

Among the multiple gap features, the distinct small gap of $\Delta=2-2.5$ meV with $2\Delta/k_BT_c=1.2-1.5$ is in fact quite unusual for the reason that the gap ratio should not be less than 3.5 for the simple BCS theory. Nevertheless this feature can be explained by the induced order parameters. Since the tunneling density of states and the T dependence of the gaps are very similar between the two band model and the proximity effect, as already stated, it is difficult to distinguish between them from the spectral fittings.[12,13] The key feature is the observation of more than two gaps with single T_c. This is incompatible with the simple isotropic two-band superconductivity. Assuming the proximity-induced gap, Δ (T) would undergo a steplike change at the reduced T_c, or continue to persist up to bulk T_c, depending on the coupling between the surface and the bulk electronic states.[12,13] In this case, the small Δ (0) and non-BCS Δ (T) in Fig. 4 could occur depending on the junction condition. The possible existence of pronounced extrema in the anisotropic gaps, as predicted by the band calculation of the extremely anisotropic Fermi surface, could also be the origin of more than two gaps with a small gap,[11] which, however, remain to be experimentally examined. Concerning the small gap, the PES revealed a small surface-derived band around Γ point in the Brillouin zone, which could be connected with the observed small gap.[23]

We further investigate the multi gaps observed here by applying the magnetic field (B), where the superconductivity is suppressed in a different way from the thermal effect.[24] Figures 5(a) and 5(b) show the tunneling conductance at various magnetic fields, which are applied perpendicular to the tunneling currents. The largest single gap is presented in (a), while the two-gap feature is shown in (b). Unfortunately, distinct gap features as in Fig. 1 are not stable when a magnetic field is applied. Therefore, the field dependence is examined with broader gaps, which are usually stable against magnetic fields. Further, we choose the data exhibiting no zero-bias peak [except for the inset of (b)], because such a leakage could cause the excessive local pair breaking owing to the current-induced field near the junction. The gap values in (b) under the fields are obtained by fitting procedures using the weighted sum of the broadened BCS density of states.[25] The apparent shift of the energies of the multigap in the field is demonstrated in the inset of (b). These apparent gap-peak positions are almost consistent with the gap energies determined by the fitting. Since MgB_2 is a type-II superconductor with the Ginzburg-Landau parameter $\kappa\sim 26$, the gap in the field probed by break-junction tunneling is assumed to be a specially averaged order parameter in the vortex states.[26] With an increasing field, the gap-edge peak shifts to lower bias accompanying the broadening. Since the Zeemann energy ($\sim$60 μeV/T) is much smaller than the gap energy, the observed gap-closing feature is attributed to the

breaking up of cooper pairs in the condensate. In Fig. 5(c), the field dependence of the gap $\Delta(B)$ is plotted up to 8 T with the expression $\Delta(B)=\Delta(B=0)[1-B/B_c]^{1/2}$ for the type-II BCS superconductor (broken curves).[26] B_c represents the gap-closing field determined from the above expression. The extrapolations using this expression for the larger gap are done on the basis of the agreement between the experimental data and calculated $\Delta(B)$ for the smaller gap. Therefore, ambiguity remains in determining B_c for the larger gap. Nevertheless, here we adopt extrapolated values because their widths apparently decrease as shown in (a), which can be fitted by the above expression of $\Delta(B)$ by choosing the appropriate B_c. In Fig. 5(d), B_c vs Δ is plotted from the fitting results in (c) and other data. The errors are mainly owing to different junctions showing the similar gap sizes. This is probably due to either the geometrical difference in the flux penetration or a possible manifestation of the gap anisotropy. The extrapolated value of $B_c \approx 18-20$ T for the $\Delta \approx 9$ meV gap is comparable to the upper-critical field 20–23 T along the *ab* plane (parallel to the Mg-B sheets) from the magnetic measurements,[15] thereby indicating that this gap is predominant to MgB_2. B_c increases with increasing Δ for $\Delta > 5-6$ meV. We can compare the behavior in (d) with the relationship $B_c = a\Delta(B=0)^2[a \approx 0.21-0.28\ \mathrm{T/(meV)^2}]$ for $\Delta > 5-6$ meV using the Ginzburg-Landau theory.[27] The approximate agreement between the above expression and the experimental data indicates that the B_c is determined by Δ (0 K) rather than T_c, violating the simple relationship $\Delta \propto T_c$. From the above coefficient $a = 2\pi^3/ehv_F^2$, the Fermi velocity is estimated to be $v_F \approx 2.4-2.8\times 10^5$ m/s, which is smaller but roughly consistent with that from the calculation.[28] Further, B_c becomes almost independent of Δ for $\Delta < 4$ meV. This can be explained by assuming the induced superconducting phase, in which the coherence length for $\Delta < 4$ meV does not become so large because of the induced small v_F. A tiny fraction of the nonsuperconducting phase distributed in the bulk MgB_2 (Ref. 16) is also a possible origin, which acts as the magnetic pinning center. It is noted that the value of $\Delta \approx 5-6$ meV in the crossover region is close to the BCS value with $T_c = 39$ K. From the above extrapolating procedures, the magnetic field distinguishes the behavior of gaps with the larger B_c for the larger Δ above ≈ 5 meV. This is in contrast to the $\Delta(T)$, where different gap sizes possess the *same* T_c. From Fig. 5, the physical properties should exhibit an anomaly at $B_c \sim 7-13$ T for the 2-meV gap. The upper critical field at 0 K along the *c* axis (perpendicular to the Mg-B sheets) ($\sim 4-8$ T) determined by the magnetic measurements is indeed not so different from the above value, but there is a certain discrepancy between them. This suggests that the 2-meV gap perhaps does not directly reflect the *c*-axis properties. On the other hand, $B_c \sim 7-10$ T for the $\sim$5-meV gap is rather close to the above upper-critical field. These facts imply that the different gap values could be classified into larger groups. Apparently, single-crystal measurements in several magnetic-field directions are necessary to find out the exact correlations between the crystallographic direction and the gap size with its suppression field B_c.

In summary, break-junction tunneling measurements of MgB_2 clarify the multigap structures distributing $\Delta \approx 2-10$ meV with $2\Delta/k_BT_c = 1.2-6$. The conductance features agree with the correlated two-gap model. The observed small gap as well as the non-BCS $\Delta(T)$ is consistent with the behavior of induced order parameters. The magnetic field reveals a higher extrapolated gap-closing field B_c for the larger gap for $\Delta > 5$ meV, but B_c becomes almost independent of Δ below 5 meV. The B_c for the largest gap $\Delta \approx 10$ meV almost agrees with the upper-critical field along the Mg-B sheets. Therefore, this gap can be predominant to MgB_2. The largest ratio $2\Delta/k_BT_c = 5-6$ well exceeds the largest strong-coupling ratio ($\sim$4.3) for the conventional inter-metallic superconductors, which deserves to study further. After finishing this work, we have found a similar conductance fitting for the induced (smaller) gap Δ_2 at low temperature.[29]

This work was supported in part by a Grant-in-Aid for COE research (No. 13CE2002) of the Ministry of Education, Culture, Sports, Science and Technology of Japan.

*Corresponding author. Email address: ekino@hiroshima-u.ac.jp

[1] J. Nagamatsu, N. Nakagawa, T. Muranaka, Y. Zenitani, and J. Akimitsu, Nature (London) **410**, 63 (2001).
[2] H. Kotegawa, K. Ishida, Y. Kitaoka, T. Muranaka, and J. Akimitsu, Phys. Rev. Lett. **87**, 127001 (2001).
[3] T. Takahashi, T. Sato, S. Souma, T. Muranaka, and J. Akimitsu, Phys. Rev. Lett. **86**, 4915 (2001).
[4] S. Tsuda, T. Yokoya, T. Kiss, Y. Takano, T. Togano, H. Kito, H. Ihara, and S. Shin, Phys. Rev. Lett. **87**, 177006 (2001).
[5] G. R. Bollinger, H. Suderow, and S. Vieira, Phys. Rev. Lett. **86**, 5582 (2001).
[6] G. Karapetrov, M. Iavarone, W. K. Kwok, G. W. Crabtree, and D. G. Hinks, Phys. Rev. Lett. **86**, 4374 (2001).
[7] F. Giubileo, D. Roditchev, W. Sacks, R. Lamy, D. X. Thanh, J. Klein, S. Miraglia, D. Fruchart, J. Marcus, and Ph. Monod, Phys. Rev. Lett. **87**, 177008 (2001).
[8] Y. Bugoslavsky, G. K. Perkins, X. Qi, L. F. Cohen, and A. D. Caplin, Nature (London) **410**, 563 (2001).
[9] X. K. Chen, M. J. Konstantinovic, J. C. Irwin, D. D. Lawrie, and J. P. Frank, Phys. Rev. Lett. **87**, 157002 (2001).
[10] J. W. Quilty, S. Lee, A. Yamamoto, and S. Tajima, Phys. Rev. Lett. **88**, 087001 (2001).
[11] A. Y. Liu, I. I. Marzin, and J. Kortus, Phys. Rev. Lett. **87**, 087005 (2001).
[12] N. Schopohl and K. Scharnberg, Solid State Commun. **22**, 371 (1977).
[13] W. L. McMillan, Phys. Rev. **175**, 537 (1968).
[14] S. Haas and K. Maki, Phys. Rev. B **65**, 020502(R) (2002).
[15] Yu. Eltsev, S. Lee, K. Nakao, N. Chikumoto, S. Tajima, N. Koshizuka, and M. Murakami, Phys. Rev. B **65**, 140501(R) (2002); M. Angst, R. Puzniak, A. Wisniewski, J. Jun, S. M. Kazakov, J. Karpinski, J. Roos, and H. Keller, Phys. Rev. Lett. **88**, 167004 (2002).
[16] R. F. Kile, J. C. Idrobo, N. D. Browning, K. A. Regan, N. S. Rogado, and R. J. Cava, Appl. Phys. Lett. **79**, 1837 (2001); R. P. Vasquez, C. U. Jung, M.-S. Park, H. J. Kim, J. Y. Kim, and S. I.

Lee, Phys. Rev. B **64**, 052510 (2001).
[17] A. Gilabert, J. P. Romagnon, and E. Guyon, Solid State Commun. **9**, 1295 (1971).
[18] B. Mitrovic, H. G. Zarate, and J. P. Carbotte, Phys. Rev. B **29**, 184 (1984).
[19] R. Osborn, E. A. Goremychkin, A. I. Kolesnikov, and D. G. Hinks, Phys. Rev. Lett. **87**, 017005 (2001).
[20] J. M. An and W. E. Pikett, Phys. Rev. Lett. **86**, 4366 (2001).
[21] T. Ekino, T. Takasaki, T. Muranaka, H. Fujii, J. Akimitsu, and S. Yamanaka, Physica B **328**, 23 (2003).
[22] T. Ekino, Y. Sezaki, and H. Fujii, Phys. Rev. B **60**, 6916 (1999); T. Ekino, S. Hashimoto, T. Takasaki, and H. Fujii, *ibid.* **64**, 092510 (2001).
[23] H. Uchiyama, K. M. Shen, S. Lee, A. Damascelli, D. H. Lu, D. L. Feng, Z.-X. Shen, and S. Tajima, Phys. Rev. Lett. **88**, 157002 (2002).
[24] A. A. Abrikosov, Zh. Eksp. Teor. Fiz. **32**, 1442 (1957) [Sov. Phys. JETP **5**, 1174 (1957)].
[25] T. Ekino, T. Takasaki, H. Fujii, T. Muranaka, and J. Akimitsu, Acta Phys. Pol. B **34**, 523 (2003).
[26] Y. G. Naidyuk, H. v. Loehneysen, and I. K. Yanson, Phys. Rev. B **54**, 16 077 (1996); T. Ekino, Y. Sezaki, and H. Fujii, *Advances in Superconductivity X* (Springer, New York, 1998), p. 183.
[27] M. Tinkham, *Introduction to Superconductivity*, 2nd ed. (McGraw-Hill, New York, 1996).
[28] J. Kortus, I. I. Mazin, K. D. Belashchenko, V. P. Antropov, and L. L. Boyer, Phys. Rev. Lett. **86**, 4656 (2001).
[29] H. Schmidt, J. F. Zasadzinski, K. E. Gray, and D. G. Hinks, Phys. Rev. Lett. **88**, 127002 (2002).